

Modelling charge self-trapping in wide-gap dielectrics: Localization problem in local density functionals

Jacob L. Gavartin, Peter V. Sushko, and Alexander L. Shluger

Department of Physics and Astronomy, University College London, Gower Street, London WC1E 6BT, UK

(Dated: May 2, 2019)

We discuss the adiabatic self-trapping of small polarons within the density functional theory (DFT). In particular, we carried out plane-wave pseudo-potential calculations of the triplet exciton in NaCl and found no energy minimum corresponding to the self-trapped exciton (STE) contrary to the experimental evidence and previous calculations. To explore the origin of this problem we modelled the self-trapped hole in NaCl using hybrid density functionals and an embedded cluster method. Calculations show that the stability of the self-trapped state of the hole drastically depends on the amount of the exact exchange in the density functional: at less than 30% of the Hartree-Fock exchange, only delocalized hole is stable, at 50% - both delocalized and self-trapped states are stable, while further increase of exact exchange results in only the self-trapped state being stable. We argue that the main contributions to the self-trapping energy such as the kinetic energy of the localizing charge, the chemical bond formation of the di-halogen quasi molecule, and the lattice polarization, are represented incorrectly within the Kohn-Sham (KS) based approaches.

I. INTRODUCTION

Despite considerable progress in studies of self-trapped excitons and polarons, the dynamics of early stages of self-trapping in specific systems is still poorly understood. The conceptual difficulty primarily lies with the fact that the quasi particle in question undergoes a transition between the free (delocalized) state and the localized one. In case of small polarons this transition is also associated with a substantial local lattice distortion. Within an adiabatic approximation one can describe self-trapping in terms of a potential energy surface (PES) connecting free and localized states. Then a microscopic model of self-trapping will involve a characterization of this PES, i.e. relevant atomic coordinates, relative energies of the free and self-trapped states, the energy barrier (if any) between them, as well as spectroscopic properties of free and self-trapped species.

Significant progress has been achieved in understanding of the conditions for polaron and exciton localization and self-trapping, as summarized in recent reviews^{1,2,3,4}. It has been suggested by Rashba⁵ that in three dimensional dielectric crystals, the free and self-trapped forms of excitons may coexist, thus implying an energy barrier separating the two states. The height of this barrier affects the dynamics and characteristic time of self-trapping process. However, atomistic modelling has only been successful in calculating the structure and properties of strongly localized systems and never in modelling transitions between delocalized and localized states. One should note that the barrier for self-trapping, if it exists, is not likely to exceed a few tenths of an electron volt². Therefore, its experimental verification and theoretical calculation is extremely challenging.

It has been anticipated that further development of quantum mechanical techniques, especially Density Functional Theory (DFT), will allow one to close this gap and achieve predictive modelling of self-trapping or defect induced trapping process. However, recent at-

tempts to calculate even well established models of small radius polarons have failed unexpectedly. Calculations of the triplet self-trapped exciton in NaCl using plane-wave DFT in the Generalized Gradient Approximation (GGA) predicted no stable state⁶ in direct contradiction with the experimental evidence² and previous Hartree-Fock calculations^{7,8}. On the other hand, Perebeinos *et al.*⁹ using plane-wave local spin density (LSDA) approach predicted the existence of a marginally stable STE in this system, albeit higher in energy than the free exciton state. Song *et al.*^{10,11,12} applied plane wave DFT to the triplet exciton in α -quartz and similarly found the free exciton state to be more stable than the localized one. The delocalized solution has also been found in LSDA calculations of the hole trapping at the Li^0 center in MgO¹³. Pacchioni *et al.*¹⁴ and Lægsgaard *et al.*¹⁵ considered the hole trapped at an Al impurity in silica. Both groups concluded that the predicted structure of this defect strongly depends on the density functional used in the calculations: local and GGA functionals predicted only the delocalized hole to be stable, again in contradiction with the experiment. Importantly, the non-local density functionals predict more localized states for this system.

An apparent bias of DFT calculations towards the delocalized electronic states was attributed to the self-interaction error inherent in the local or semilocal GGA type approximations, which are central to the Kohn-Sham method¹⁶. It is unclear, however, to what extent the local approximation affects qualitative results (localized versus delocalized states), and what is the role of other factors in the calculation, such as boundary conditions, basis set completeness, and pseudopotential approximation.

In this paper, we consider a triplet exciton and a hole in the archetypal ionic insulator NaCl. These defects have been studied extensively both experimentally and theoretically^{2,7,17} and thus provide good test systems. Previous calculations were carried out mainly in small

embedded cluster models using the Hartree-Fock method and therefore were unable to treat delocalized states and take full account of the electron correlation. We would like to model a transition from delocalized to self-trapped exciton state and for this purpose use the plane-wave DFT method. We analyse the effect of size of a periodic supercell and the related question of spurious multipole interactions in this system and conclude that no stable self-trapped state for the exciton or a hole is predicted within the GGA DFT framework, once these factors are eliminated. To separate the localization problem from the effects of periodic boundary conditions (PBC) we then consider a hole within the embedded cluster approach and find that the non-local contribution to the exchange interaction is decisive in the description of self-trapped states.

The paper is organized as follows. In the next Section we give a brief account of the microscopic models of the self-trapped exciton and hole in alkali halides. Next we outline the details of the periodic plane-wave and embedded cluster procedures used. The results of calculations for an exciton and a hole are presented respectively in Sections IV and V, followed by discussion in section VI.

II. SELF-TRAPPED EXCITON AND HOLE IN ALKALI HALIDES: BACKGROUND

Most of the alkali halides at normal pressure and temperature assume the face centered cubic structure (Fig. 1a) (except cesium halides which are simple cubic). Self-trapped excitons (STE) and holes in these crystals exhibit the features of both molecular and dielectric polaron character. In particular, the self-trapped hole (otherwise called a V_k -center) is known to be localized on two adjacent halogen ions forming a X_2^- molecular ion (Fig. 1d). There is no experimental evidence pointing to existence of a barrier for the hole self-trapping in alkali halides^{2,18}, suggesting that the free hole is unstable. In particular, Lushchik¹⁹ *et al.* estimated that the mean free path of a free hole in NaCl before self-trapping does not exceed $30 a_0$ (a_0 is the shortest Na-Cl distance in the perfect lattice). The hole self-trapping energy, which is the difference between the energies of the fully delocalized and localized states, is larger than the activation energy for the V_k center diffusion (~ 0.4 eV in NaCl)²⁰. Therefore, it is expected that the description of such a deep state is well within the reach of the DFT theory.

The model and the geometric structure of the V_k -center in alkali halides has been first proposed on the basis of the analysis of the electron spin resonance data^{21,22} and later refined in numerous theoretical calculations^{17,23,24,25}. The structure and stability of the V_k -center is primarily determined by the chemical bond formation between the two halogen ions, assisted by the lattice polarization.

Self-trapped triplet excitons in alkali halides can be formed either directly by excitation in the exciton band or as a result of recombination of electron with a self-

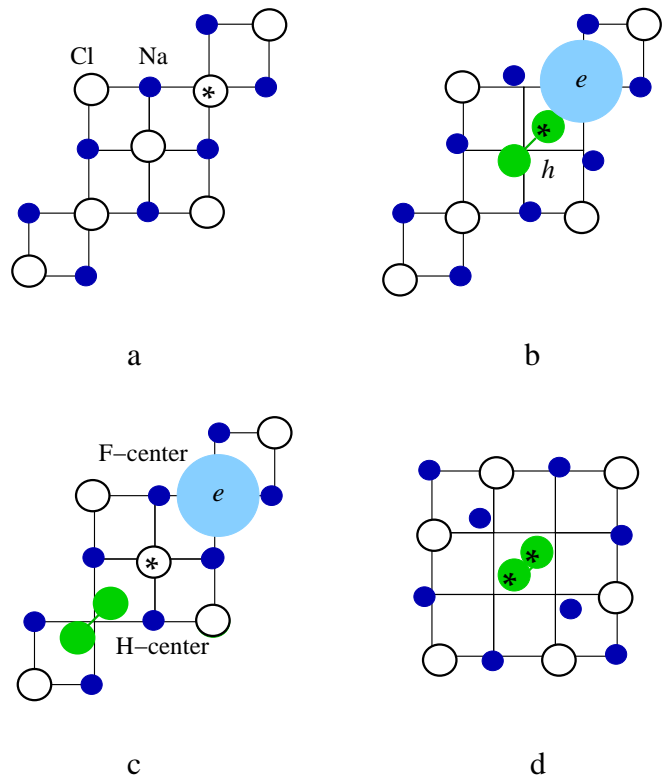


FIG. 1: Schematic representations of the perfect rock-salt structure (a); of the triplet self-trapped exciton (b), the closest separated F-H pair (c), and the V_k -center (d) in an alkali halide crystal. The marked atoms were constrained during the optimization procedure.

trapped hole, V_k -center. It is currently accepted that the STE in alkali halides consists of a hole localized on the X_2^- molecular ion, and an electron localized in its vicinity. The so-called on-center and off-center configurations of triplet STE are considered in the literature². In the on-center configuration the X_2^- molecular ion equally occupies two nearest anion sites (as in Fig. 1d), with the electron cloud symmetrically localized around it and has the D_{2h} point symmetry group. It is therefore called a $(V_k + e)$ configuration. Williams and Song²⁶ suggested that in some alkali halides at least, the on-center configuration of the STE is unstable relative to an off-center displacement of the X_2^- ion along the $\langle 110 \rangle$ crystallographic direction towards one of the anion sites (Fig. 1b). The center of mass of the electron component in this configuration is localized near the other (vacant) anion site, thus giving the C_{2v} symmetry to the STE. This model of the triplet STE in alkali halides has been further developed using effective potential and embedded cluster *ab initio* Hartree-Fock calculations, as reviewed by Song and Williams². The STE in NaCl has also been studied using *ab initio* embedded cluster methods by Puchin^{7,27} *et al.*, who confirmed the existence of the off-center STE configuration and demonstrated the importance of the electron correlation in determining the properties of the

STE.

Triplet STE created by irradiation may subsequently annihilate (radiatively or non-radiatively) restoring the perfect lattice, or decay into a Frenkel pair of lattice defects: an electron in an anion vacancy (F-center) and an interstitial halogen atom in the form of an X_2^- molecular ion occupying one halogen site, the H-center, (Fig. 1c). The energy barrier between the off-center STE and the closest F-H pair has been calculated in alkali chlorides and bromides by Song et al.²⁸ and also recently in KBr by Shluger and Tanimura⁸. The dissociation barrier for the STE is found to be very low (0.07 eV for NaCl and 0.03 eV for KBr)²⁸. The activation energy for the STE diffusion in NaCl is somewhat larger²⁰ ~ 0.13 eV.

At the outset of this work we hoped to use the plane wave periodic DFT methods to treat both delocalized and localized states and to study the adiabatic potential for self-trapping of triplet exciton in NaCl. The results presented below highlight the limited applicability of the existing functionals to the localization problem.

III. CALCULATION PROCEDURE

A. Periodic DFT calculations

In order to model the triplet exciton self-trapping we consider the adiabatic coordinate corresponding to a displacement, Δ , of one chlorine ion (hereafter designated as Cl^*) along the $\langle 110 \rangle$ crystalline axis with all other surrounding atoms²⁹ relaxed at each position of the Cl^* . The displacement Δ is measured in units of $1/8$ of the plane diagonal ($a_0\sqrt{2}$). By virtue of construction, the specified adiabatic coordinate connects the free exciton state ($\Delta = 0$) (Fig. 1a) with the STE configuration ($\Delta \sim 4 - 5$) (Fig. 1b), and the closest F-H pair separated by one lattice anion, $\Delta \sim 8$) (Fig. 1c). The considered potential energy surface (PES) allows for both on- and off-center forms of STE as well as for the transient one-centre excitons proposed by Shluger and Tanimura⁸. However, it should be emphasised, that an existence of the potential energy barrier along this coordinate does not rule out a possibility of alternative self-trapping paths with still lower energy barriers.

The PES along the coordinate Δ was calculated using the plane-wave density functional approach implemented in the VASP code³⁰ with the GGA density functional due to Perdew and Wang³¹ and the ultra-soft pseudopotentials³² as supplied by Kresse and Hafner³³. The self-consistent triplet excited state was modelled by constraining the total spin of the system to $S=1$, so as to obtain the lowest energy state of given multiplicity.

To study the effect of the super-cell size, the exciton PES was calculated in unit cells containing 32, 64, 108 and 144 ions. The details of the super-cells are given in Table I together with the sets of k-points used and number of atoms explicitly relaxed. At each position of Cl^* the specified ions were relaxed, so that the maximum

TABLE I: The supercells used in the exciton calculations, specified by the number of atoms, Cartesian translation vectors (given in units of the shortest Na-Cl distance a_0) and the number of irreducible k-points used in the calculations. The last column shows the value of the optimized lattice constant a_0 for the ground and excited states.

Atoms (relaxed) ²⁹	Translation vectors (a_0)	No k-points	a_0 Å	
			s=0	s=1
2	(1 1 0), (1 0 1), (0 1 1)	35	2.845	-
32 (26)	(4 0 0), (0 4 0), (2 2 2)	4	2.83	2.87
64 (48)	(4 0 0), (0 4 0), (0 0 4)	4	2.84	2.85
108 (28)	(3 3 0), (3 0 3), (0 6 6)	3	2.83	2.84
144 (46)	(6 0 0), (0 6 0), (0 0 4)	1	2.84	2.84

force acting on any individual atom did not exceed 0.04 eV/Å²⁹. Most of the calculations were performed with an energy cut-off of 285 eV.

As shall be seen below, the calculated PES for the exciton self-trapping does not display a minimum for the STE. Furthermore, the shape of PES strongly varies with the size of the supercell. In order to separate the effects of the boundary conditions and density functionals, we considered the formation of the V_k -center in NaCl using an embedded cluster method implemented in the GUESS code^{34,35}.

B. Embedded cluster calculations

In this method, a crystal is represented by a large finite nano-cluster, that is divided into several regions. Spherical region I at the centre of the nano-cluster includes a quantum-mechanically treated cluster (QC) surrounded by interface ions and a region of classical shell model ions³⁶. The remaining part of the nano-cluster is represented by classical non-polarizable ions. All quantum mechanical, interface and classical ions (both cores and shells) in region I are allowed to relax simultaneously in the course of geometry optimization. Ions outside region I remain fixed and provide an accurate electrostatic potential within region I. This approach allows one to take into account the defect-induced lattice polarization of a crystal region containing a few hundred atoms. An account of lattice polarisation outside region I can be extended to infinity using a polarizable continuum model and the Mott-Littleton approach³⁷. In this approximation the polarization energy is proportional to the square of the excess charge in the lattice. In the case of the V_k -center, the charge remains constant, so the Mott-Littleton contribution cancels out in any energy differences. Therefore this term was neglected in the current calculations.

The described scheme is implemented in the GUESS code^{34,35}, which provides an interface between the GAUSSIAN package³⁸ for calculation the electronic structure of the QC and a code providing the shell model

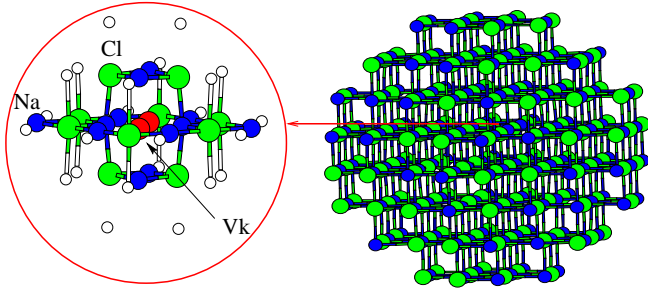


FIG. 2: Illustration of the embedded cluster model used in the V_k -center calculation (only region 1 is shown). The quantum cluster is shown enlarged. The small white balls represent the sodium interface atoms

representation of the rest of the crystal. The total energy and the electronic structure of the QC is calculated by solving standard Hartree-Fock or Kohn-Sham equations which include the matrix elements of the electrostatic potential due to all classical point charges in regions I and II computed on the basis functions of the cluster. Further details for the total energy evaluation in this approach are given elsewhere³⁴.

A cubic nano-cluster containing 8000 (20x20x20) ions was used in these calculations. Spherical region I of radius 11.5 Å included 300 ions and a stoichiometric QC comprising 22 ions (Fig. 2).

In our scheme, the charge density in QC interacts with the classical atoms only electrostatically, which results in artificial polarization by the classical cations nearest to the QC³⁹. To avoid this, an interface region between the QC and classical ions in region I was introduced. In the present model it includes 20 Na ions represented by effective core pseudopotentials⁴⁰, and a single s -type basis function (see Fig. 2). Therefore all QC anions are fully coordinated by either quantum or interface ions. For the quantum cluster we have used an all electron Gaussian type atomic basis⁴¹ optimized for the NaCl crystal (8 – 511 G for Na and 86 – 311 G for Cl).

The shell model ions in region I interact via pair potentials due to Catlow *et al.*⁴², which were slightly modified to represent more accurately the static dielectric constant. Modified potentials give a static equilibrium $Na - Cl$ distance of 2.79 Å and fairly well reproduce the elastic, dielectric and phonon properties of the perfect NaCl crystal.

The embedded cluster calculations were carried out using three different density functionals: the Hartree-Fock, Becke hybrid three parameter (B3), and so-called half-and-half functionals (BH&H)⁴³. The latter two incorporate 20% and 50% of the Hartree-Fock exchange, respectively⁴³. The hybrid exchange functionals were used in conjunction with the Lee, Yang and Parr cor-

relation functional (LYP)⁴⁴.

Consistency of the interactions between the classical and quantum regions was tested by calculating an ideal QC embedded into an ideal classical lattice. The optimized $Na - Cl$ distances inside the QC and those at the cluster boundary differ from the $Na - Cl$ distances in the rest of the nano-cluster by *ca.* 1% and 3.5% respectively.

IV. EXCITON SELF-TRAPPING IN NaCl

Exciton self-trapping is associated with a strong lattice relaxation. It has been suggested that this relaxation is associated with the significant volume change⁴⁵. To account for this effect, we optimized the lattice constant of the supercells in both the ground and excited triplet states using the VASP code. The results are presented in (Table I). The calculated ground state equilibrium lattice constant $a_0 = 2.84$ Å is $\sim 2\%$ larger than the experimental value, extrapolated to 0 K, of 2.79 Å. We also observe a slight increase of the perfect lattice constant in the triplet excited state in smaller supercells.

Next, we calculate the potential energy surface for the triplet exciton by displacing a selected Cl^* ion along the $\langle 110 \rangle$ crystallographic axis and relaxing all the surrounding atoms at each Cl^* position (Fig. 1a,b,c). The PES for the triplet state calculated in different supercells is shown in Figure 3. Additional information on the lattice relaxation and spin density changes along the Cl^* displacement coordinate can be found on our webpage⁴⁶. It is seen that the obtained PES varies significantly with the size and shape of the supercell, in which it was calculated. In all calculations the free exciton configuration is predicted to be the lowest energy state, as reported previously^{6,9}. The off-center STE configuration corresponds approximately to ($\Delta \sim 5$). This state is predicted to be marginally stable only in the smallest supercell used (identical to the one used by Perebeinos *et al.*⁹). We also observe that the energy difference between the free exciton and the expected self-trapped state increases with the size of the supercell.

We have singled out most probable causes of the significant dependence of the calculated PES on the size and shape of different supercells: i) defect volume change; ii) spurious electrostatic interaction between the supercells; iii) basis set completeness, and iv) pseudopotential approximation. In the rest of this Section we discuss these aspects.

To mimic the effect of the volume change associated with the self-trapping, we optimized the volume of the 144 ion supercell at each point of the adiabatic surface. The equilibrium lattice constant, a_0 has increased only slightly: from 2.840 Å for a perfect lattice ($\Delta = 0$) to 2.848 Å at the expected STE state ($\Delta = 5$). The total energy of the STE has lowered by ~ 0.1 eV and the energy minimum for the STE did not exist.

As can be seen in (Fig. 1b), the charge distribution in off-center STE is associated with a substantial dipole mo-

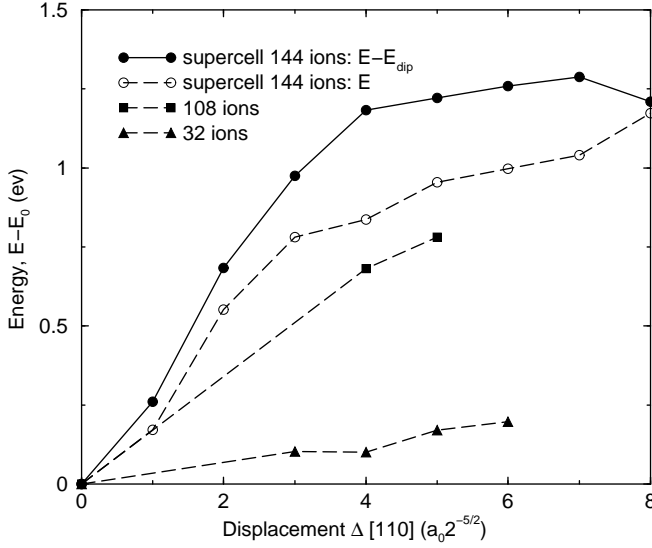


FIG. 3: The potential energy surface for the triplet exciton as described in the text. The energies are plotted with respect to the energies of the triplet state of a perfect lattice (zero coordinate). $\Delta \sim 5$ corresponds to the expected minimum for the STE (Fig. 1b), $\Delta = 8$ corresponds to the next nearest-neighbour F-H pair (Fig. 1c). The dipole corrected (solid line) and uncorrected (dashed line) energies are shown for the supercell of 144 ions.

ment. The strong dependence of the PES on the supercell size suggests that a significant contribution to the total energy can arise from the interaction between periodic dipoles persisting even for comparatively large supercells. The dipole-dipole interaction energy resulting from the super-lattice of dipoles can be evaluated according to the expression⁴⁷:

$$E_{dip} = -\frac{2G^3}{3\sqrt{\pi}}\mathbf{P}^2 + \frac{1}{2}P_\alpha T_{\alpha\beta} P_\beta, \quad (1)$$

where Einstein notation is adopted for the sums over repeated indices, P_i denotes the Cartesian component of the dipole vector \mathbf{P} , G is the Ewald parameter, and

$$T_{\alpha\beta} = \frac{4\pi}{v_c} \sum_{g \neq 0} \frac{R_{g\alpha} R_{g\beta}}{R_g^2} e^{-R_g^2/4G^2} - G^3 \sum_{i \neq 0} H_{\alpha\beta}(\mathbf{G}\mathbf{R}_i). \quad (2)$$

Here the first sum is over the reciprocal lattice vectors \mathbf{R}_g and the second - over the direct lattice vectors \mathbf{R}_i with the zero vector ($i = 0$) being excluded to avoid self-interaction. In addition, $H_{\alpha\beta}(\mathbf{y}) = -\delta_{\alpha\beta}H(y) + y_\alpha y_\beta / y^2 [3H(y) + 4/\sqrt{\pi}e^{-y^2}]$ and $H(y) = 2\sqrt{\pi}y^{-2}e^{-y^2} + \text{erfc}(y)/y^3$. Equation (1) is a generalization of the Makov and Payne formula⁴⁸ for the non-cubic supercells.

To quantify the dipole-dipole interaction energy the dipole moment of the supercell needs to be calculated. For a neutral periodic system this must be defined as an invariant of a coordinate system⁴⁹:

$$\mathbf{P}(\mathbf{r}) = \Omega^{-1} \int_{cell} \mathbf{r} \rho(\mathbf{r}) d^3\mathbf{r} + \Omega^{-1} \int_{surface} \mathbf{r} [\mathbf{n} \boldsymbol{\Pi}(\mathbf{r})] ds, \quad (3)$$

where the first integral is taken over the volume of the supercell, and the second over the supercell surface, Ω is the volume of the supercell, $\rho(\mathbf{r})$ is a charge density (including both electronic and atomic cores), \mathbf{n} is an outward surface-normal unit vector, and $\boldsymbol{\Pi}$ is a local polarization defined via the equation:

$$\nabla \boldsymbol{\Pi}(\mathbf{r}) = -\rho(\mathbf{r}). \quad (4)$$

It should be noted, that within the PBC only the whole sum in Eq. 3 is an invariant with respect to the coordinate origin. However, the second integral there can be made small by an appropriate choice of a coordinate system. Then and only then the dipole moment of the supercell can be correctly estimated by the first integral in Eq. (3). To minimize the contribution of the surface integral we chose the supercell as a Wigner-Seitz cell, where the origin of the charge density grid is located not on an atomic site, but on a volume interstitial position in the face centered cubic lattice.

The Cartesian components of the calculated dipole moment for each atomic configuration of the exciton along the adiabatic coordinate, Δ , in the supercell of 144 atoms are shown in Fig. 4. The dipole moment varies non-monotonically along the Δ coordinate reaching a maximum near the expected STE configuration. Thus, the PES corrected for the dipole-dipole interaction may in principle contain a local minimum for the STE. To explore this possibility we calculated the value of the dipole energy (Eq. 1) in different unit cells for the expected STE configuration ($\Delta = 5$). For that we assumed that calculations in different unit cells yield approximately the same charge density for the STE and used the value for the dipole moment, \mathbf{P} , calculated in the 144 supercell for $\Delta = 5$ (Fig. 4). The obtained values of E_{dip} are equal to -4.85, -2.64, 0.18, and -0.27 eV for the 32, 64, 108, and 144 ion supercells, respectively, and are negative except for the 108 ion supercell. This difference is caused by the fact that this supercell has a rhombohedral shape whereas the other cells are rectangular.

From the tendency shown in Fig. 4, we expect that the $E_{dip}(\Delta = 5)$ values given above represent the largest corrections for different supercells. When subtracted from the total energy, $E(\Delta) - E_{dip}(\Delta)$, they in most cases enhance even further the difference between the free and off-center STE energies. The full PES corrected by the dipole-dipole contribution, $E(\Delta) - E_{dip}(\Delta)$, was calculated only for the largest 144 ion supercell where the correction is the smallest (see Fig. 3). Although the shape of the PES changes slightly, it does not show a minimum for any displacement Δ . It is also clear that no energy minimum for the STE will occur in the 32 ion supercell after the dipole correction is taken into account. Our calculations clearly demonstrate that spurious electrostatic interaction in small unit cells may result in an artificial energy minimum for the STE. We suggest that the marginally stable STE configuration in the 32 atoms supercell reported by Perebeinos⁹ *et al.* and also found in our calculation is precisely of this origin.

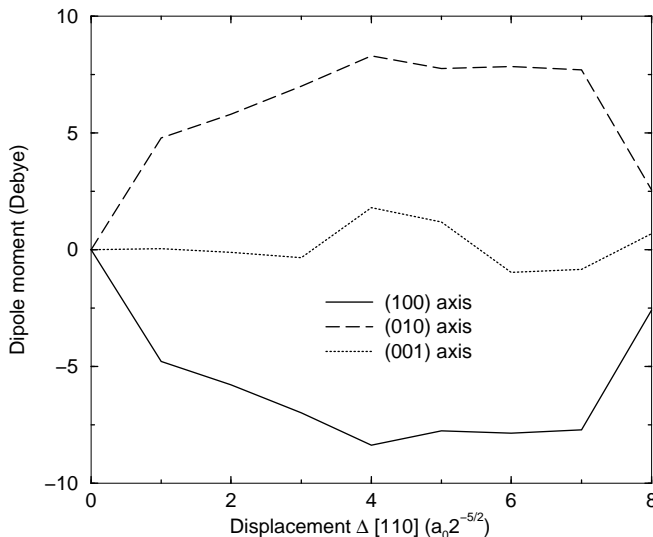


FIG. 4: The electric dipole moment as a function of the adiabatic coordinate Δ , remaining details as in Fig. 3

We should note that the E_{dip} calculated using Eq. (1) overestimates the electrostatic interaction between the supercells in PBC due to various approximations in Eq. (1) :

1. The point dipole approximation assumed in Eq. (1), breaks down whenever the dipole length is comparable with the supercell size. (Hence unrealistically large dipole energies are obtained in small supercells).

2. Eq. (1) does not account for a dielectric screening.

3. The higher multipole contributions (dipole-quadrupole etc.) would generally have the sign opposite to E_{dip} and may reduce the overall effect of spurious multipole interactions.

4. Due to a strong multipole interaction in smaller supercells, the charge distributions, and therefore the dipole moments, predicted in different supercells may differ significantly.

In spite of these remarks we believe that further refinement of the calculations will not affect the main conclusion - no stable state for the STE is predicted by the GGA DFT approach.

The reasons for the absence of a STE energy minimum in the local DFT approximation are not obvious. Several factors could result in the bias towards the delocalized solution. These include, for example, the choice of energy cut-off and k-point sampling. To check these issues, we compared calculations with cut-off energies of 220 eV and 285 eV and observed no significant difference in the STE relaxation. The k-point sampling is likely to affect more the energies of delocalized states. In fact we do observe a slight increase of the free exciton energy with the number of irreducible k-points. This reduces the energy difference between the free and the self-trapped exciton, though the minimum for the STE still does not arise. Another uncontrolled factor in the calculation is the pseudopotential approximation for core electrons. In particu-

lar, we employed a large core ($1s^2 2s^2 p^6$) pseudopotential for sodium atoms and the polarization of cations was virtually neglected in our calculations. To examine the role of cation polarization, we carried out the STE calculations with the Helium core pseudopotential for Na atoms for selected configurations in the 64 atoms supercell. This also did not affect our qualitative conclusions - no energy minimum was obtained for the STE.

Our analysis suggests that the problem of localization lies not with the technical details of the calculations but rather more fundamentally with the approximations involved in the GGA density functional. In particular, essentially uncontrolled self-interaction error in the local density approximation is the most likely cause. However, a detailed characterisation of the involved energy terms is difficult for the exciton, which comprises two strongly interacting spins with the energies near the top of the valence band and the bottom of the conduction band respectively. It must be emphasised at this point that holes in alkali halides do self-trap in the form of V_k -centres, while the electrons do not. Hence, the hole self-trapping is also fundamental in the exciton localization. At the same time, self-trapping of the hole is a simpler problem in that it involves localization of a single spin. However, being charged, a hole presents some difficulty for studying within the PBC. In particular, we obtained no self-trapping of the hole within plane wave DFT. Therefore, we resorted to modelling the hole within the embedded cluster method, that has the following advantages: 1. The atomic-type basis set ensures no bias towards the delocalized states; 2. The lattice polarisation effects paramount for charged polar systems are fully accounted for; 3. The use of the atomic basis sets allows the straightforward application of a number of local and non-local density functionals, so that the properties of various functionals can be studied.

V. HOLE TRAPPING IN NACL

The calculations of the hole (a total charge of the system is equal to +1) were performed within the embedded cluster model discussed in Section IIIB (Fig. 2). We calculated the total energy of the system as a function of the distance between the two Cl ions equally displaced along the $\langle 110 \rangle$ axis towards each other from their respective perfect lattice sites (see Fig. 1d). All other ions in region I were relaxed simultaneously to their equilibrium positions for each Cl-Cl separation.

The potential energy surfaces calculated with different density functionals are depicted in Fig. 5. The zero energy in the top panel corresponds to the singly ionized perfect lattice calculated within each method. We observe that the shape of PES qualitatively depends on the amount of the Hartree-Fock exchange included in the density functional. The B3LYP functional predicts one global minimum corresponding to a free hole, the BH&H functional predicts two minima separated by a marginal

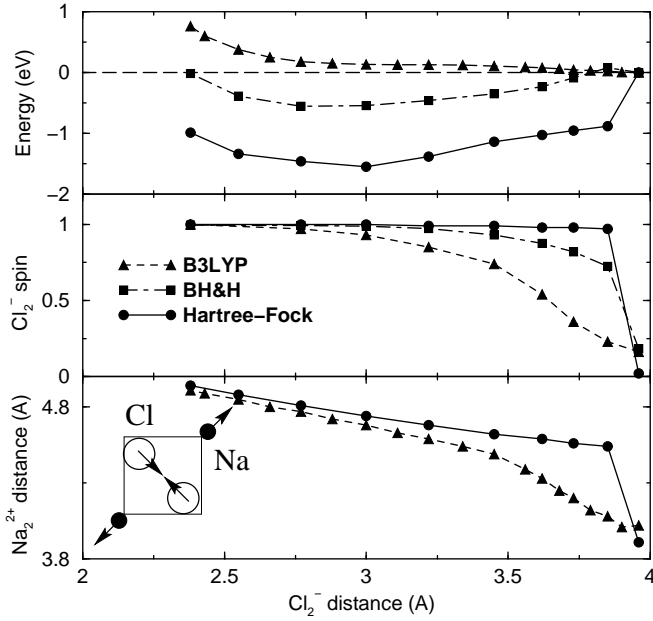


FIG. 5: The adiabatic surface for the V_k -center (top panel), calculated with various density functionals. At each given Cl_2^- distance, all other atoms in the system were relaxed to the minimum energy geometry. Zero energy corresponds to the perfect crystal configuration (the extended hole). The middle panel shows the dependence of the Mulliken spin population on the Cl_2^- molecule as a function of the same adiabatic coordinate. The bottom panel shows the relaxation of the pair of Na atoms adjacent to the V_k -center.

barrier, while the Hartree-Fock method gives a single energy minimum corresponding to the self-trapped hole (V_k -center) (top panel of Fig. 5). Furthermore, the energy difference between the free and self-trapped states ranges between -0.2 eV for B3LYP and 1.5 eV for the HF.

Different functionals also predict distinctly different spin localization. The analysis of the Mulliken spin population on the Cl_2^- molecule (middle panel in Fig. 5) reveals that the extent of spin localization increases faster with decreasing Cl_2^- distance when the amount of exact exchange is larger. In particular, the Hartree-Fock calculations predict the spin almost fully localized on Cl_2^- at a mere 0.05 Å displacement of two Cl ions from their respective lattice sites. The B3LYP functional, on the contrary, predicts very gradual spin localization with the decrease of the Cl-Cl distance. The variance in localization of spin in different functionals also affects the lattice relaxation. The bottom panel in Figure 5 shows the distance between the two relaxed Na ions adjacent to the Cl_2^- molecule as a function of the Cl_2^- distance. It is seen that weak spin localization predicted in the B3LYP functional causes much smaller cation relaxation than that obtained in the Hartree-Fock method.

VI. DISCUSSION

Our results highlight severe problems with applying density functional theory to the self-trapping problem. The LSDA and GGA density functionals yield solutions biased towards the delocalized states to such an extent that no stable self-trapped state is predicted for either a hole or an exciton, contrary to experimental evidence.

Let us emphasise that the degree of localisation of a polaron is closely linked to the properties of the single particle spectrum for the problem. For instance, spin density of the V_k -center is represented almost entirely by the single-particle density of the last occupied orbital in a majority spin, $\psi_s(\mathbf{r}')$. The degree of localization of $\psi_s(\mathbf{r}')$ is related to its energy, ϵ_s , or more precisely, to the energy split of the ϵ_s from the corresponding band edge. In the KS method, ϵ_s is defined as¹⁶:

$$\epsilon_s = \langle \psi_s | -\frac{1}{2}\nabla^2 + v_{eff}(\mathbf{r}) | \psi_s \rangle, \quad (5)$$

where

$$v_{eff}(\mathbf{r}) = v(\mathbf{r}) + \int \frac{\rho(\mathbf{r}')}{|\mathbf{r} - \mathbf{r}'|} d\mathbf{r}' + v_{xc}(\mathbf{r}). \quad (6)$$

Here, $v(\mathbf{r})$ represents the external potential of the atomic cores, the second term is the classical electrostatic potential due to electrons of density $\rho(\mathbf{r})$, (including the self-interaction), and $v_{xc}(\mathbf{r})$ is a local exchange-correlation potential, where the self-interaction energy is partially cancelled. How do the terms in Eq. (5) contribute into self-trapping? One of the main factors facilitating self-trapping is lattice polarization. In alkali halide crystals, the second (and perhaps dominant) negative term is the energy gain due to the formation of the σ -bond (localised doubly occupied orbital) in the X_2^- molecular ion ($X = \text{F, Cl, Br, I}$). The factors favouring self-trapping are partially counterbalanced by an increase in the kinetic energy of localizing electrons. The latter results in a splitting of corresponding single particle levels from the edge of the valence band. First, we note that any perturbation in the external potential, $v(\mathbf{r})$, alone cannot cause self-trapping, since it does not depend on the number of electrons or their state, and self-trapping does not occur in a neutral crystal in its ground state. This is in contrast to polaron localization by defects, where the $v(\mathbf{r})$ contribution to localization is dominant. Therefore the critical localization terms for self-trapping are contained in the Hartree (electronic polarisation) and exchange-correlation (bond formation) terms.

Apparently, an accurate calculation of these contributions presents a serious problem for the KS DFT, for the following reasons:

1) First, let us consider the formation of the X_2^- quasi-molecule. For that purpose we calculate the dissociation curve for the free Cl_2^- molecular ion using different density functionals and the Gaussian-98 package³⁸. We shall use as a reference the energy curve obtained by the coupled cluster method with double substitutions (CCD).

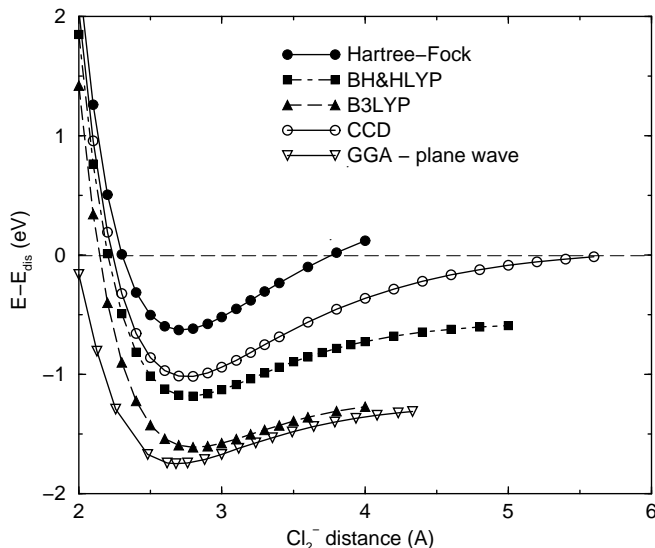


FIG. 6: The dissociation curve for the Cl_2^- molecular ion calculated using various density functionals ($E_{dis} = E(Cl^-) + E_{Cl^0}$). All the local basis calculations are done using the G86-311 Gaussian basis set⁴¹. In the plane wave GGA calculations the energy cut-off 285.3 eV is used.

In Fig 6, we observe that both the Unrestricted Hartree-Fock and all studied DFT functionals do not predict the correct dissociation behaviour for this open shell ion. Moreover, local as well as hybrid density functionals (but not the Hartree-Fock method) violate the energy variational principle in that the predicted dissociation curves asymptotically tend to energies significantly lower than the corresponding dissociation limit (i.e. the sum of the ground state energies of the isolated negative chlorine ion and the neutral chlorine atom). The implication of this drawback for the self-trapping is clear - the energy gain associated with a decrease of the inter-ionic distance in the Cl_2^- from ~ 4 Å (as in a perfect lattice) to the V_k -center equilibrium configuration (~ 3 Å), is substantially underestimated by the DFT and overestimated by the UHF method.

Incorrect dissociation behaviour of radical ions in DFT was first reported by Bally and Sastry⁵⁰. The subsequent comprehensive analysis of the H_2^+ molecular ion by Zhang and Yang⁵¹ revealed that the self-interaction error in local density functional for such systems becomes uncontrollably large. It can be demonstrated that the self-interaction error, associated with the single particle states, is positive and increases with their localization. Therefore, self-interaction, being minimized during self-consistency, will also lead to the less localized single particle states.

2) The polarization properties of a many electron system in the density functional theory are related to the exchange-correlation kernel⁵² $K_{xc}(\mathbf{r}, \mathbf{r}') = \frac{\delta^2 E_{xc}}{\delta n(\mathbf{r}) \delta n(\mathbf{r}')}$. The exact exchange correlation kernel is shown to possess the so-called ultra-non-locality property, i.e. the diago-

nal element of its Fourier transform $K(\mathbf{q}, \mathbf{q})$ possesses a $O(1/q^2)$ divergence at small wavenumbers q . However, as first demonstrated in refs.^{52,53}, both LDA and GGA lead to $K_{xc}(\mathbf{r}\mathbf{r}')$ which does not have the required $O(1/q^2)$ divergence. One of the implications of the non-divergent exchange-correlation kernel in KS DFT is that the macroscopic polarizability of the system (calculated as a KS polarizability) depends on the number of electrons and on the occupancy of the KS bands. That is, a calculated KS polarizability of the dielectric will be generally different in a singlet and triplet state, and for a system with or without the hole (both systems are technically metallic). Thus, the reliability of polarization contribution in KS DFT for the triplet or charged systems is also essentially uncontrolled.

3) As mentioned earlier, the largely single particle character of the self-trapping problem implies that the total spin density may be represented by a single particle density of just one orbital. It is known however, that KS orbitals do not necessarily carry this physical meaning. In particular, by virtue of construction, the KS formalism yields the single particle eigenstates which minimize the kinetic energy (as calculated on single particle orbitals)¹⁶. Thus, the kinetic energy contribution is always underestimated, leading generally to the least localized set of orbitals for a given density. Another delocalizing factor is the self-interaction error in the Hartree term, which is only partially cancelled in the local approximations to the exchange-correlation potentials. Apparently, a positive self-interaction grows uncontrollably as the state becomes more and more localized. Therefore, any self-consistent procedure minimizing the total energy, also minimizes self-interaction by delocalizing the orbitals. It should be noted, that the effects of minimization of the kinetic energy and self-interaction in KS method have the same effect and cannot be separated, since any form of non-local self-interaction correction leads to the single particle equations distinct from those of KS.

Conceivably the depth of the self-trapping potential in polar dielectrics is unlikely to exceed 1 eV. It seems, that the spurious delocalizing contributions inherent in the KS method always outgrow the localizing potential, so the self-trapped state cannot be predicted in this approach.

This problem is partially resolved by use of hybrid density functionals. We have demonstrated for the holes that the self-trapped solution gradually becomes energetically more stable as the amount of the exact exchange is increased. However, the conventional hybrid functionals, such as B3LYP, failed to predict a stable V_k -center, let alone its localization energy. This raises the question of parametrisation strategies for semiempirical functionals, which are not clear in the context of self-trapping.

Our calculations also highlighted another important methodological issue related to the calculations of the PES for polar systems within the periodic boundary conditions. The artificial multipole electrostatic interactions between supercells may drastically affect the shape of the PES, if the leading multipoles of the charge density vary

along the chosen adiabatic coordinate. The dipole-dipole interaction in the triplet exciton modelled in a small supercell resulted in the appearance of the energy minimum for the STE configuration reported by Perebeinos *et al.*⁹. Interestingly, the authors of ref.⁹ reported that no stable configuration could be found for the V_k -center. These results can be understood by recalling that in the V_k -center calculations the leading term in the electrostatic interaction between the supercells is the monopole-monopole one. This term does not vary with the adiabatic coordinate and therefore does not affect the shape of the PES.

Although artificial delocalization in KS based DFT theory can be expected, it is difficult to assess *a priori* when a specific functional will fail in practical calculations. We suggest, that the problem with the localized states in KS method will occur in all cases where the localization potential is provided mainly by the electron-electron term. These include self-trapping phenomena, Jahn-Teller systems, low dimensional systems (e.g. Pierls instability), and systems with weak impurity perturbations. A list (by no means complete) of problematic DFT calculations where an artificial delocalization was reported includes: the hole localization in CaO doped with Li and Na and the F-center in LiF as reported by Dovesi *et al.*¹³; dimerization in C_{4N+2} carbon rings⁵⁴; the structure of the Al defect in α -quartz^{14,15,55}; exciton self-trapping in presence of thermal disorder^{6,56}; the phase diagram of crystalline Pu (related to a localization of f -type atomic orbitals)^{57,58,59}.

On the other hand, the use of the Hartree-Fock based approaches is also limited since neglecting electron correlation favours localized states⁶⁰. One should also note that frequently used approaches based on tight binding methods do not fully account for the electron kinetic energy, and thus are also intrinsically biased towards localized solutions. As seen from these arguments, the DFT approach in KS formalism is unable to reliably resolve between localized and delocalized situations in systems where both type of states are possible. A more adequate many-electron theory for the self-trapping problem must go beyond the KS methods. Different forms of the density functionals free of the self-interaction error should be examined.

Acknowledgments

The authors gratefully acknowledge funding by the Leverhulme Trust and NATO grant CRG.974075. Calculations have been performed on the CRAY T3E supercomputer facility provided by the Materials Chemistry Consortium, UK, and on the Bentham computer at the HiPerSpace Centre at the University College London. JLG is grateful to A. Sokol for many stimulating discussions, and to E. Kotomin, E. Heifets, L. Kantorovich, G. Pacchioni, and C. Bird for their useful comments on the manuscript.

-
- ¹ E. I. Rashba, *Excitons* (Oxford University Press, 1989).
 - ² K. S. Song and R. T. Williams, *Self-Trapped Excitons* (Springer-Verlag, Berlin, 1993).
 - ³ A. L. Shluger and A. M. Stoneham, J. Phys.: Condens. Matter **5**, 3049 (1993).
 - ⁴ A. L. Shluger, J. L. Gavartin, M. A. Szymanski, and S. A. M., Nucl. Instr. Meth. B **166-167**, 1 (2000).
 - ⁵ E. Rashba, Opt. Spektrosk. **2**, 75 (1957).
 - ⁶ J. L. Gavartin and A. L. Shluger, Rad. Eff. Def. Solids **155**, 311 (2001).
 - ⁷ V. E. Puchin, A. L. Shluger, and N. Itoh, Phys. Rev. B **52**, 6254 (1995).
 - ⁸ A. L. Shluger and K. Tanimura, Phys. Rev. B **61**, 5392 (2000).
 - ⁹ V. Perebeinos, P. B. Allen, and M. Weinert, Phys. Rev. B **62**, 12589 (2000).
 - ¹⁰ J. Song, H. Jónsson, and L. R. Corrales, Nucl. Instr. and Meth in Phys. Res. B **166-167**, 451 (2000).
 - ¹¹ J. Song, R. M. VanGinhoven, L. R. Corrales, and H. Jónsson, Faraday Discuss. **117**, 303 (2000).
 - ¹² J. Song, L. R. Corrales, G. Kresse, and H. Jónsson, Phys. Rev. B **64** (2001).
 - ¹³ R. Dovesi, R. Orlando, C. Roetti, C. Pisani, and V. R. Saunders, Phys. Status Solidi B **217**, 63 (2000).
 - ¹⁴ G. Pacchioni, F. Frigoli, D. Ricci, and J. A. Weil, Phys. Rev. B **63**, 0241XX (2001).
 - ¹⁵ J. Lægsgaard and K. Stokbro, Phys. Rev. Lett. **86**, 2834 (2001).
 - ¹⁶ R. G. Parr and W. Yang, *Density-Functional Theory of Atoms and Molecules* (North-Holland, Amsterdam, 1982).
 - ¹⁷ A. Testa, A. M. Stoneham, C. R. A. Catlow, K. S. Song, A. H. Harker, and J. H. Harding, Rad. Effects and Defects in Solids **119**, 27 (1991).
 - ¹⁸ E. D. Aluker, D. Y. Lysis, and S. A. Chernov, *Electronic excitations and radioluminescence in alkali halide crystals* (Riga, Zinatne, 1979).
 - ¹⁹ C. B. Lushchik and A. C. Lushchik, *Decay of electronic excitations with defects formation in solids* (Moscow, Nauka, 1989).
 - ²⁰ K. Tanimura and N. Itoh, J. Phys. Chem. Solids **42**, 901 (1981).
 - ²¹ T. G. Castner and W. Känzig, J. Phys. Chem. Solids **3**, 178 (1957).
 - ²² D. Schoemaker, Phys. Rev. B **7**, 786 (1973).
 - ²³ L. Kantorovich, E. Heifets, L. Livshicz, M. Kuklja, and P. Zapol, Phys. Rev. B **47**, 14875 (1993).
 - ²⁴ A. L. Shluger, L. N. Kantorovich, E. N. Heifets, E. K. Shidlovskaya, and R. W. Grimes, J. Phys.: Condens. Matter **4**, 7417 (1992).
 - ²⁵ A. L. Shluger, V. E. Puchin, T. Suzuki, K. Tanimura, and N. Itoh, Phys. Rev. B **52**, 4017 (1995).
 - ²⁶ C. H. Leung, G. Brunet, and K. S. Song, J. Phys. C: Solid State Phys. **18**, 4459 (1985).
 - ²⁷ V. E. Puchin, A. L. Shluger, and N. Tanimura, K. Itoh, Phys. Rev. B **47**, 6226 (1993).
 - ²⁸ K. S. Song, C. H. Leung, and R. T. Williams, J. Phys.:

- Condens. Matter **1**, 683 (1989).
- ²⁹ In the supercell of 32 atoms, the 6 most remote atoms from the exciton were constrained. In the supercell of 64 atoms, atoms located in the (100) plane most remote from and parallel to the (100) plane of the exciton were constrained during the geometry optimisation. All other atoms were relaxed. In the supercells containing 108 and 144 atoms, all the atoms on which the force exceeded $0.04 \text{ eV}\text{\AA}^{-1}$ were included in the relaxation.
 - ³⁰ G. Kresse and J. Furthmüller, Phys. Rev. B **54**, 11169 (1996).
 - ³¹ J. P. Perdew and Y. Wang, Phys. Rev. B **46**, 12947 (1992).
 - ³² D. Vanderbilt, Phys. Rev. B **41**, 7892 (1990).
 - ³³ G. Kresse and J. Hafner, J. Phys.: Condens. Matter **6**, 8245 (1994).
 - ³⁴ P. V. Sushko, A. L. Shluger, and C. R. A. Catlow, Surf. Sci. **450**, 153 ((2000)).
 - ³⁵ P. V. Sushko, A. L. Shluger, R. C. Baetzold, and C. R. A. Catlow, J. Phys.: Condens. Matter **12**, 8257 (2000).
 - ³⁶ B. G. Dick and A. W. Overhauser, Phys. Rev. **112**, 90 ((1958)).
 - ³⁷ C. R. A. Catlow and A. M. Stoneham, J. Chem. Soc. Faraday. Trans. 2 **85** (1989).
 - ³⁸ M. J. Frisch, G. W. Trucks, H. B. Schlegel, G. E. Scuseria, M. A. Robb, J. R. Cheeseman, V. G. Zakrzewski, J. A. Montgomery, R. E. Stratmann, J. C. Burant, et al., *GAUSSIAN 98 (Release A1)*, Pittsburgh PA (1998).
 - ³⁹ A. M. Ferrari and G. Pacchioni, J. Phys. Chem. **107**, 2066 ((1997)).
 - ⁴⁰ W. R. Wadt and P. J. Hay, J. Chem. Phys. **82**, 284 ((1985)).
 - ⁴¹ M. Prencipe, A. Zupan, R. Dovesi, E. Aprà, and V. R. Saunders, Phys. Rev. B **51**, 3391 (1995).
 - ⁴² C. R. A. Catlow, K. M. Diller, and M. G. Norgett, J. Phys. C: Solid State Phys. **10**, 1395 (1977).
 - ⁴³ A. D. Becke, J. Chem. Phys. **98**, 5648 (1993).
 - ⁴⁴ C. Lee, W. Yang, and R. G. Parr, Phys. Rev. B **37**, 785 (1988).
 - ⁴⁵ K. Tanimura, T. Tanaka, and N. Itoh, Phys. Rev. Lett. **51**, 423 (1983).
 - ⁴⁶ J. L. Gavartin (1999), URL <http://www.cmp.phys.ucl.ac.uk/~jlg/Exciton/anm.html>.
 - ⁴⁷ L. N. Kantorovich, Phys. Rev. B **60**, 15476 (1999).
 - ⁴⁸ G. Makov and M. C. Payne, Phys. Rev. B **51**, 4014 (1995).
 - ⁴⁹ R. M. Martin, Phys. Rev. B **9**, 1998 (1974).
 - ⁵⁰ T. Bally and G. N. Sastry, J. Phys. Chem A **101**, 7923 (1997).
 - ⁵¹ Y. Zhang and W. Yang, J. Chem. Phys. **109**, 2604 (1998).
 - ⁵² X. Gonze, P. Ghoses, and R. W. Godby, Phys. Rev. Lett. **74**, 4035 (1995).
 - ⁵³ P. Ghoses, X. Gonze, and R. W. Godby, Phys. Rev. B **56**, 12811 (1997).
 - ⁵⁴ T. Torelli and L. Mitás, Phys. Rev. Lett. **85**, 1702 (2000).
 - ⁵⁵ M. Magagnoli, P. Gianozzi, and A. D. Corso, Phys. Rev. B **61**, 2621 (2000).
 - ⁵⁶ J. L. Gavartin and A. L. Shluger, Phys. Rev. B **in print** (2001).
 - ⁵⁷ P. Soderlind, O. Eriksson, B. Johansson, and J. M. Wills, Phys. Rev. B **50**, 7291 (1994).
 - ⁵⁸ M. D. Jones, J. C. Boettger, R. C. Albers, and D. J. Singh, Phys. Rev. B **61**, 4644 (2000).
 - ⁵⁹ S. Y. Savrasov, G. Kotliar, and E. Abrahams, Nature **410**, 793 (2001).
 - ⁶⁰ P. Fulde, *Electron Correlations in Molecules and Solids. 3rd ed.* (Springer, Springer Series in Solid State Sciences 100, 1995).